



Enhancement of wool fabric dyeing via treatment with AgNPs

Hayam M. Ahmed*, Asrar G. Emam

Chemistry Department, Faculty of Science, Al-Azhar University (Girls), Nasr City, Cairo, Egypt



Abstract

Nanoparticles are a successful material for fibers and textiles functionality. In this work, silver nanoparticles (AgNPs) were synthesized by the chemical reduction of Ag⁺ and then the AgNPs were investigated by UV-visible (UV-vis) spectrophotometer, transmission electron microscopy (TEM), scanning electron microscopy (SEM) and Fourier transform infrared spectroscopy (FTIR). The synthesized nanoparticles were used for the surface improvement of the fabric, and the fabric was then dyed with C.I. Acid Red 18 (AR 18) at different temperatures. The physical properties, tensile strength, wrinkle rate, color strength, and colorfastness to perspiration of wool fabric were studied in dyed wool and raw wool fabric. It was found that the nanoparticle-treated fiber was stronger than untreated yarn. The corresponding rate of adsorption was analyzed and calculated according to different kinetic models. Furthermore, diffusion coefficients, the activation energy, and thermodynamic parameters were calculated. Treatment with AgNPs produces a wool fabric with excellent color fastness and antibacterial properties enables enhanced health care and reduced environmental impacts.

Keywords: Dyeing; Wool; Nanomaterials; Modified fiber; Acid dye; Antimicrobe

Introduction

Azo-acid dyes are main organic acids, ordinarily in the semblance of salts that are available to the dyer. Generally, they are added to fiber from solutions that contain sulfuric, formic, or acetic acids. Although most of these are aromatic sulfonic acid (RSO₃Na) sodium salts, there are a few carboxylic groups. These dyes are anionic and water-soluble in general because of the involvement of sulfonic groups (SO₃⁻) in the chemical structure [1]. Azo acid dyes that are water-soluble anionic colors are mainly used to nitrogenous fabrics as nylon, silk, and wool, all contain fundamental groups. These have a wide range of colors, ranging from yellow to black, all of which are extremely brilliant [2].

Wool is one of the most significant fibers in the textile industry and, because of its unique properties such as fullness, elasticity handle, warmth retention, and comfort. It is commonly used in the

manufacture of high-quality textiles [3]. Wool has been used for clothing, blankets, horse rugs, saddle cloths, carpeting, insulation and upholstery, wool felt covers piano hammers, and it is used to absorb odors and noise in heavy machinery and stereo speakers. Increasing environmental issues and requests for ecologically responsible textile industry have led to the creation of new innovations, including using nanotechnology [4]. Nanotechnology is a promising and fast-growing area for its wide applications in different science and technology sectors [5]. Nano-size metals such as silver, platinum, and gold are widely used in medicinal applications. Among these metals, AgNPs have attracted great attention from researchers in the last two decades [6]. Nanoparticles confer multiple functionalities to textiles that are continued after repeated washing [7–9].

The nanoparticles are used for a wide variety of applications, with many safety and deficiencies in

*Corresponding author e-mail: ha_ahmed@azhar.edu.eg; (Hayam M. Ahmed).

Receive Date: 24 October 2020, Revise Date: 21 November 2020, Accept Date: 29 November 2020

DOI: 10.21608/EJCHEM.2020.47516.2968

©2021 National Information and Documentation Center (NIDOC)

ked to the nanoparticles as recently checked and published [10]. However, silver has been found to be one of the safe antibacterial agents capable of destroying harmful microorganisms, and to be non-toxic to the human body, while, exposure to silver compounds can cause toxic effects, including liver and kidney damage, eye irritation and other effects [11]. Wool is a natural protein fiber and is a good medium in which various microorganisms are able to grow. Hence, treatment with effective antibacterial agents is required through methods in international standards [12]. Silver in the shape of both ions and nanoparticles and their compounds is well-known as an antibacterial agent and extremely toxic to microorganisms. Silver salt is usually used to provide the antibacterial effect required, but when AgNPs are used, the surface area exposed to microbes is substantially increased [13]. Compared with silver ions, AgNPs are increasingly used because of their slower dissolution rate, which results in a continuous release of silver ions [14]. Several chemical methods have been published in recent years for the creation of AgNPs. The prepared of AgNPs by the reduction process involves the effect of a reduction agent and concentration of surfactants. However, a major reason for the large use of chemical reduction is its simplicity. This method also allows for variability in the molar concentration of the reactant, dispersant, and feed rate and thus creates AgNPs with regulated particle sizes, shapes, and size distribution. The selection of an effective reduction agent is also major factor because the particle size distribution, shape, and size depend heavily on the nature of the reduction agent [15].

The main objective of this study was to use the chemical reduction procedure to synthesize AgNPs from Ag ions. Then, the wool fabric was functionalized and adjusted by surface treatment with the prepared AgNPs. Kinetic enhancement of the dyeing properties of NP-treated wool fabric with AR 18 was performed by increasing the dye affinity through the modification of several dyeing process parameters, and we studied the effect of AgNPs treatment on the tensile strength, wrinkle percentage, color power, colorfastness to perspiration, and antibacterial properties of the treated wool fabric.

2. Materials and Methods

2.1. Materials

The wool textile (provided by the Miser Helwan Company) was 140 g/m², 36 threads/cm warp, 30/1 yarn count, 34 threads/cm weft, and 30/1 yarn count. Natural acid dye (C.I. Red acid 18), silver nitrate (AgNO₃), sodium sulfate decahydrate

(Na₂SO₄ · 10 H₂O) and trisodium citrate (Na₃C₆H₅O₇ · 2H₂O) were used, as well as a simple stock solution of C.I. Red Acid 18 at 1 g/L concentration.

2.2. Methods

2.2.1. Preparation of AgNPs

The chemical reduction process was used to prepare AgNPs [16]. The solutions were prepared in deionized water. Using a hot plate magnetic stirrer, 50 mL of silver nitrate at 0.001 M was heated to boil. Drop by drop, 5 mL of 1% trisodium citrate was applied to this solution. During this process, the solution was vigorously combined. The solution was heated until a change in color (yellowish-brown) was visible, after which heating was stopped, and the solution was left to cool at room temperature.

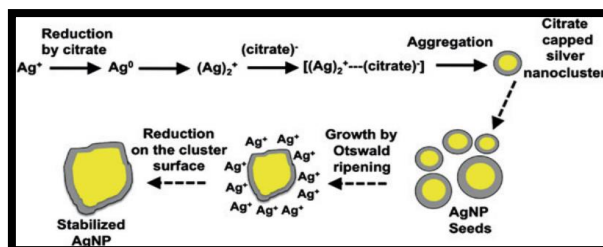


Fig. 1. Schematic representation of the nucleation and growth mechanism for AgNPs prepared by the citrate method according to Pillai [17].

2.2.2. Treatment of wool fabric using (AgNPs)

The surface modification of wool fabrics with AgNPs was carried out by the dip-coating process via stirring. Briefly, 1 g of wool fabric was dipped in a solution containing 0.25 g of Ag nanoparticles in water and subjected to vigorous stirring for 2 h at 300 rpm with boiling. The Ag-coated fabric was then withdrawn from the solution and cleaned with water to separate residual AgNPs from the surface. The resulting fabric was dried at ordinary temperature [17].

2.2.3. Dyeing process of untreated and treated wool fabric with AR 18

Easy laboratory dyeing method was used to dye both untreated and AgNPs treated wool fabrics with AR18 in a liquor ratio of 1:50. The fabric was submerged in a dye-bath containing 50 mL of 100 mg/L dye solution, 10 mL of 30% sodium sulfate decahydrate, 99% H₂SO₄ (drops were used to adjust the pH of the dye bath) and stirred for 15 min. Then, the bath temperature was raised to 50, 75, or 90°C over 30-40 min after that time, another 5 mL of sodium sulfate decahydrate was added and dyeing

continued at these temperatures (50, 75, or 90°C) for a maximum of 120 min. The wool fabrics were then cooled to room temperature and washed with an aqueous solution of a nonionic detergent (2 g/l) at 40°C for 10-15 min [18]. Fig. 2 shows photos of AgNPs treated wool fabrics before dyeing and after dyeing at different temperatures. The optimum conditions of dyeing were 100 mg/L of dye, pH = 2.8 to 3.0, temperature = 90°C and dyeing bath time = 2 h. The percentage of wool shrinkage due to high temperature is very low before treatment and almost neglected after treatment.

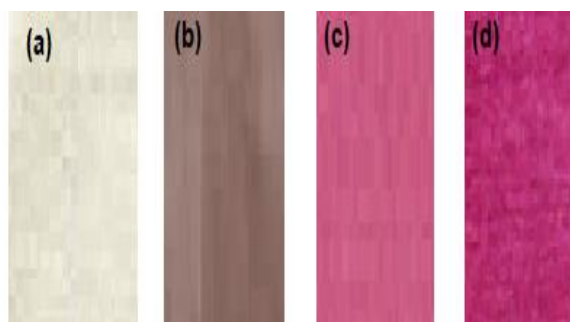


Fig. 2. AgNPs treated wool fabrics; before dyeing (a), after dyeing at 50°C (b), 75°C (c) and 90°C (d).

2.2.3.1. Color measurements

Color intensity (K/S values) is evaluated by light reflectance measurements using spectrophotometer, K/S was determined using the Kubelka–Munk equation [19]:

$$K/S = \frac{(1-R)^2}{2R} - \frac{(1-R^0)^2}{2R^0}$$

Where R and R⁰ are the decimal fractions of the reflectance of the colored and uncolored fabrics, respectively; K is the absorption coefficient, and S is the dispersing coefficient.

2.2.3.2. Fastness properties

The processed dyed specimens were examined using standard ISO techniques. The basic measurements were made for colorfastness for washing under ISO105-C02 (1989), for sudden colorfastness under ISO105-E04 (1989), and for colorfastness against light (carbon arc) under ISO105-B02 (1988).

2.2.3.3. Tensile strength

Some specimens were taken from the wool fabrics for the tensile strength tests. Tests of the specimens were conducted on a Sintech worldwide mechanical tester

with a load cell weighing 1113N (250 lb) according to ASTM technique D-5035. The length of the gauge taken was 5 cm, and the speed of the crosshead was established to 50 mm/min. At least 20 yarns were removed and checked for each fabric sample.

2.2.3.4. FTIR Spectroscopy Measurement

To study and identify functional groups of the pre- and post-adsorption samples, infrared transform spectroscopy (FTIR) was used. KBr powders were used to detect FTIR spectra ranging from 400-4000 cm⁻¹ (Mattson 1000, Unicam infrared spectrophotometers).

2.2.3.5. Scanning electron microscope, SEM

Using SEM (JEOL JSM-5400 SEM-Tokyo, Japan) at 20 kV, the surface morphology of AgNPs was characterized. Prior to SEM, the surface of particles was sputter-coated with gold using a JEOL FRC 1200 fine coater to improve the sample conductivity, and the samples were observed by scanning. The chemical composition of AgNPs was analyzed using surface Energy dispersive X-ray spectroscopy (EDX) (EDAX AMETEK analyzer) attached with the electron microscope.

2.2.3.6. Transmission electron microscope (TEM)

To characterize the AgNPs, TEM measurements were acquired (JEOL JEM-1010-Tokyo, Japan) at 200 kV with a sensitivity point of 0.45 nm. The AgNPs were dispersed in ethanol, and then a drop of the above disperse was taken for TEM imaging on a carbon-coated copper grid (300 meshes).

2.2.3.7. UV–VIS Spectroscopy

Using a UV–VIS spectrophotometer instrument, the concentration of the dye solution was measured for dyed specimens by measuring absorbance at λ_{max} (model T60 spectrophotometer, UK).

2.2.4. Dyeing kinetics

For untreated and treated wool fabrics dyed with AR18, kinetic studies were conducted for periods varying from 10 min to 2 h in dye basin. The liquor ratio was maintained at 1:50, and the temperature was slowly increased to 50, 75, and 90°C. All colored specimens were immersed with water at room temperature and dried. After dyeing the fabrics, the dye concentration in aqueous solutions was determined by UV–VIS spectrophotometer (Shimadzu 1800) at λ_{max} = 495 nm, and q_t, the amount of dye adsorbed on mass unit of wool fabric, was calculated at different periods using the following equation:

$$q_t = (C_o - C_t) \frac{V}{m} \quad (1)$$

Where C_o is the actual dye concentration in the aqueous solution, C_t is the dye concentration in the aqueous solution after time t , V is the volume of dye taken; m is the total weight of wool fabric. In order to improve the reliability of the experiments, each error bar is based on three independent measurements.

The percentage of exhaustion (%E) was calculated using Equation (2).

$$\%E = \frac{(C_o - C_e)}{C_e} \cdot 100 \quad (2)$$

Where C_e is the concentration of dye at time equilibrium.

The following equations were used to evaluate the kinetic behavior of the dyeing process. Pseudo-first and second-order models [20-22] were used to investigate the mechanism of dye adsorption to the wool fabric at different temperatures:

Pseudo-first-order kinetic model

$$\ln(q_e - q_t) = \ln q_e - k_1/t \quad (3)$$

The half adsorption time ($t_{0.5}$) was calculated from the pseudo-first-order model using $t_{0.5} = 0.693/k_1$. k_1 (min^{-1}) is pseudo first order rate constant.

Pseudo-second-order kinetic model

$$\frac{t}{q_t} = \frac{1}{k_2 q_e^2} + \frac{t}{q_e} \quad (4)$$

k_2 (mg/g.min) is the rate constant of pseudo-second-order adsorption, q_e is the equilibrium adsorption capacity (mg/g) and q_t is the adsorption capacity at time t . Then, the original adsorption rate was measured by :

$$h_i = k_2 q_e^2$$

If pseudo-second-order kinetics is acceptable, a linear relationship will appear in the (t/q_t) vs. t chart. Interception and slope of (t/q_t) vs. t were used to measure the constant pseudo-second-order rate

($k_2 \text{mg/g.min}$) and the sum of equilibrium adsorption (q_e), where ($h_i \text{mg/g.min}$) is the original adsorption rate and ($k \text{mg/g.min}$) is the maximum rate constant [23, 24].

The adsorption half – life ($t_{0.5}$) was determined using [25]

$$t_{0.5} = \frac{1}{k_2 q_e}$$

Other kinetic models, such as intraparticle propagation (Eq. 5) and Elovich (Eq. 6) models can be used to the dyeing rate:

$$q_t = k_p t^{0.5} + C \quad (5)$$

Where C denotes the intercept, and k_p is the intraparticle rate constant.

$$q_t = \frac{1}{\beta} \ln(\alpha \beta) + \frac{1}{\beta} \ln t \quad (6)$$

Where α is the primary adsorption rate (mg/g.min), and β is the adsorption constant (g/mg) during any one experiment.

2.2.5. Propagation Coefficient and energy activation

The propagation coefficient from Hill's linearized was calculated [26].

$$\frac{C_t}{C_e} = 4 \left(\frac{D_t}{\pi r^2} \right)^2 \quad (7)$$

Where C_t is the dye concentration in solution at time t , C_e is the dye concentration in solution at equilibrium (mg/L), D is the propagation coefficient (cm^2/min), and r is the radius of the cylindrical fiber (cm). The propagation activation energy was estimated from the Arrhenius equation below [27]:

$$\ln D_T = \ln D_o - \left(\frac{E_a}{RT} \right) \quad (8)$$

is the propagation coefficient at a given temperature (cm^2/min), D_0 is a constant, E_a is the energy of activation, R is a gas constant (2 cal/mol K), and T is the absolute temperature (K). E_a can be calculated from the plots of $\ln D_T$ vs. $1/T$.

2.2.6. Thermodynamic studies

The following equation was used to measure thermodynamic variables such as standard affinity ($\Delta\mu^0$), dyeing entropy (ΔS^0), and enthalpy (ΔH^0) [28, 29].

$$-\Delta\mu^0 = RT \ln \frac{D_f}{vD_s} = RT \ln K_d \quad (9)$$

Where $-\Delta\mu^0$ is the standard affinity (kJ/mol), and $[D_f]$ and $[D_s]$ are the dye concentration in the fiber (mg/g) and in solution (mg/mL), respectively.

$$K_d = \frac{C_o - C_e}{C_o} \left(\frac{V}{m} \right) \quad (10)$$

$$\ln K_d = \frac{\Delta S^0}{R} - \frac{\Delta H^0}{R T} \quad (11)$$

where K_d is the distribution coefficient, C_o and C_e are the initial and final concentration of the dye solution (g/L), respectively, V (mL) is the volume, m is the mass of the wool fabric (g), R is a gas constant (8.314 J/mol. K), and T is the absolute temperature (Kelvin). The variables ΔH^0 and ΔS^0 were calculated from the slopes and intercepts of the linear plot of $\ln K_d$ versus $1/T$, respectively.

2.2.7. Antibacterial tests

To ensure reproducibility, all tests of antibacterial activity were performed in triplicate. Treated and untreated wool fabrics were tested to assess antibacterial activity against Gram-positive bacteria such as *Staphylococcus aureus* (*S. aureus*) and Gram-negative bacteria such as *Escherichia coli* (*E. coli*). All of the plates were incubated for 24 h at 37°C and examined to determine whether inhibition zones were created around fabric.

3. Results and Discussion

3.1. Characterization of AgNPs

Characterization of AgNPs is important for understanding and controlling the synthesis and application of nanoparticles. Specific methods were used to evaluate different parameters. Studies on the nanoparticle size, morphology, and composition were performed by transmission and scanning electron

microscopy, energy-dispersive spectroscopy, and X-ray diffraction.

3.1.1. UV-visible spectroscopy

UV-visible spectroscopy is one of the most common techniques for structural characterization of AgNPs. The light yellow-brown silver absorption spectrum (Fig. 3), prepared using Turkevich's method [16], shows a surface plasmon absorption band with a maximum of 425 nm , suggesting the formation of spherical or approximately spherical AgNPs. With the addition of citrate anions, particle aggregation could be prevented. Owing to the adsorbed citrate ions, AgNPs form a negative frame. The repulsive force of those spheres that are negatively charged prevents further aggregation. The absorption spectra were recorded after two weeks and after four weeks to ensure the stability of the AgNPs. The absorption spectrum did not change after even four weeks of storage (Fig. 3).

3.1.2. Transmission and scanning electron microscopy

TEM (Fig. 4a) was used to determine the size of AgNPs, and the distribution sizes of AgNPs ranged from around 5 to 50 nm . The diameter of most particles (99.2%) was less than 10 nm , although a few particles were larger. This suggests that the synthesized AgNPs had a small diameter distribution, with an average diameter of around 10 nm [30]. The TEM and SEM images (Fig. 4a and b) show that the AgNPs were spherical, with sizes ranging from 5 to 50 nm , and Figs. 4 c and d, show SEM images of untreated wool and AgNPs-treated wool. It can be clearly seen that AgNPs were distributed on the fiber surface and that the smoothness improved compared with the untreated wool surface [31].

3.1.3. Energy-dispersive spectroscopy (EDX)

Using EDX on SEM, elemental analysis of AgNPs was performed. Fig. 5 displays the EDX spectrum of the spherical nanoparticles. The peaks around 3.20 , 3.50 , and 3.70 keV correspond to the $\text{AgL}\alpha$, $\text{Ag L}\beta$, and $\text{Ag L}\beta_2$ binding energies, respectively, while the carbon peak at around 1.0 keV was observed [32]. The carbon value was the inverse of the SEM finder grid. No apparent peaks indicative of impurities were found in the scanning spectrum of binding energies. The test results suggest that the as-synthesized AgNPs had high purity.

3.1.4. Fourier transforms infrared spectroscopy (FTIR)

Fig. 6a displays the FTIR spectrum of AgNPs prepared with sodium citrate. The absorption peak

attributable to carbonyl stretching in the citrate group is located from 1695 cm^{-1} to 1615 cm^{-1} (peak 3). Other observed bands at 2858 cm^{-1} (peak 4) and 2930 cm^{-1} (peak 5) are attributable to C–H bond asym and sym stretching vibrations, and the band at 3440 cm^{-1} (peak 6) is attributable to the –OH group of H_2O [33]. The oxygen in a polar group has a strong affinity for silver ions and silver nanoparticles. AgNPs are formed by coordinative bonding between the carboxyl oxygen atom and silver [34, 35]. A blue shift of the absorption band appears at 1487 and 1389 cm^{-1} (peak 1, 2). This band displacement corresponds to the coordination of carbonyl oxygen with silver particles [33]. Fig. 6b demonstrates the comparison of the treated and untreated wool fabric using FTIR. The principal functional groups in wool are –COOH,

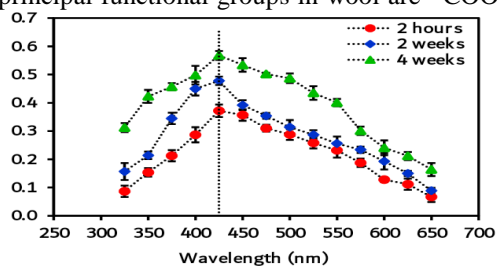
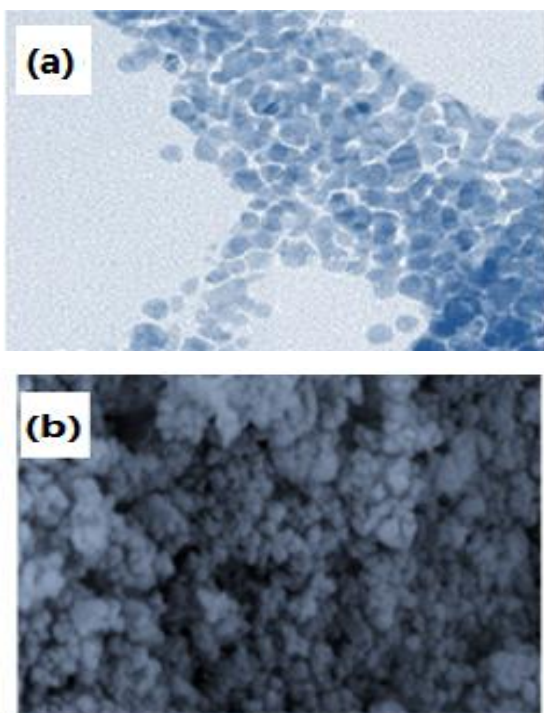


Fig. 3. UV-vis absorption spectrum of prepared AgNPs.



–NH₂, and –OH. The peaks at 3450.47 cm^{-1} (peak 10) and 1624.78 cm^{-1} (peak 6) are attributed to the –NH or –OH stretching vibration and carbonyl stretching vibrations in wool proteins depend on their chemical context, the existence of intra- or intermolecular hydrogen bonds, and amide forms. The bands at 2911.55 cm^{-1} (peak 9), 885.27 cm^{-1} (peak 3), 1216.05 cm^{-1} (peak 5), and 1050.28 cm^{-1} (peak 4) can be designated to CH stretching vibrations, CH₂ out-of-plane bending, C–O–C asym stretching, and S–O–S (cysteine monoxide), respectively [36]. In the case of AgNPs-treated wool, the CO₂ band shifted to 1614.45 cm^{-1} , while the peaks at 3450.47 and 1216.05 cm^{-1} shifted to 3415.66 and 1181.23 cm^{-1} as a result of metal ring stretching.

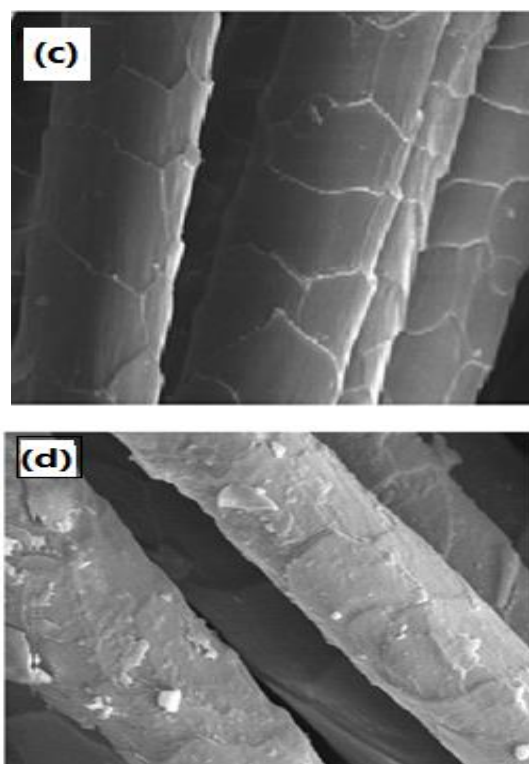


Fig. 4. (a) TEM image and (b) SEM image of spherical AgNPs; (c) SEM image of untreated wool; (d) SEM image of wool loaded with AgNPs

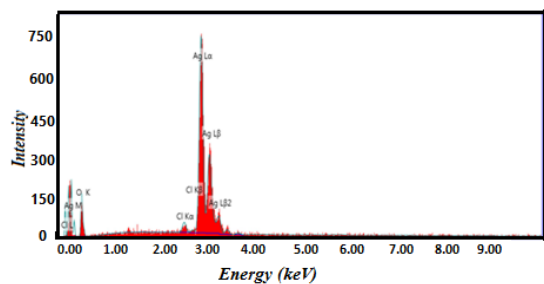


Fig. 5. EDX analysis of AgNPs

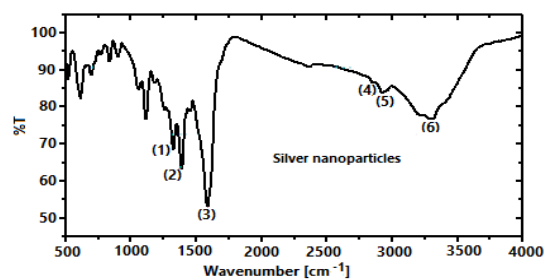


Fig. 6a. FTIR spectra of AgNPs.

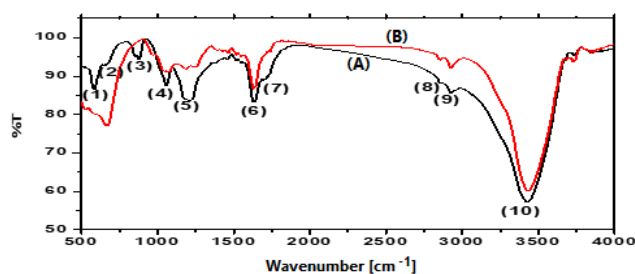


Fig. 6b. FTIR spectra of (A) untreated wool and (B) wool treated with AgNPs.

3.2. Influence of the application of AgNPs on the physical properties of the wool fabric

The effects of AgNPs treatment on the tensile strength, crimp rate, color strength, and colorfastness to perspiration of wool fabric were studied.

3.2.1. Tensile strength and wrinkle %

Table 1 reveals that the incorporation of AgNPs into the fiber structure led to an improvement in the fiber's load-bearing capacity. Due to their small size, AgNPs can fill spaces between molecules and can act as a filler or overlapping agent that contributes to the load-sharing phenomenon during the applied of load on the material [37]. In comparison to the chemical crosslinking, which improves the crease recovery angle at the expense of imparting some rigidity to the material, depending on the degree of crosslinking, the incorporation of nanosilver particles remains very gentle in this respect. The explanation for the wrinkle loss in wool fabric is that those subjected to chemical processing exhibit extreme mechanical behavior, such as padding and relaxation. The % wrinkled wool fabric was noted at different levels. A wrinkle

shrinkage tester at the national research center investigated the wrinkle % and wrinkle recovery of wool fibers. Table 2 shows that the wrinkle loss percentage of dyed fabric treated with AgNPs was higher than that of untreated wool fabric.

3.2.2. Colour measurements of treated and untreated dyed wool fabric

The AgNPs were applied to improve wool fabrics properties. After dyeing the wool with AR 18, the values of color intensity were evaluated for both AgNPs-treated and untreated wool fabric. Table 3 shows that the K/S color intensity values and colorimetric measurements (CIE L* a* b*) of treated wool are higher than those of untreated wool. The higher values of color intensity K/S (table 3) for nanoparticle-treated fabric suggest that the existence of nanometal particles increased the affinity of the dye to the fiber. Thus, AgNPs were behaving as mordants in the fabric [38]. The dye negative charged anions get attracted to the wool fiber probably due to the polarity developed in the metal particles by induction, which in turn leads to better bonding

between the fiber and the dye [38]. As shown in table 3, AgNPs pretreatment not only improved the wool color intensity but also improved its color fastness.

3.3. Dyeing kinetics

3.3.1. Dye exhaustion %

To establish the effects of dye fatigue on wool samples, three different temperatures (60, 75, and 90 °C) and three different dye concentrations (50, 100, and 150 mg/L) were applied to the wool. Fig. 7(a-c) shows the dye exhaustion isotherms obtained by dyeing untreated and treated wool fabrics at different temperatures and at dye concentrations (50, 100, and 150 mg/L) respectively. It can be seen in Fig. 7 that the exhaustion of the dye was very rapid in the first 40 min and then achieved equilibrium. The figure shows that AR 18 dyeability of the treated wool

fabric was generally better than that of the untreated under the same conditions. Dyeing exhaustion at 90 °C improved to 69.92% in a short time (25 min) for the treated fabric compared with 22.82% (in 60 min) for the untreated one. This is due to the ability of AgNPs to form a thin layer on the wool fabric during the treatment. The thin layer of AgNPs increased wool hydrophobic properties and resulted in the appearance of micro- and nanoscopic architecture on the surface, maximizing and accelerating the dye's adhesion to the surface of the wool fabric. The Lotus effect is derived from the concept of creating hydrophobic surfaces [39]. Higher temperatures led to higher exhaustion of dye in fabrics; therefore, the adsorption of dye was an endothermic process which is in agreement with previous literatures [40].

Table 1. Tensile strength (Newton/cm²) of untreated and AgNPs-treated wool fabrics (Temp. 90 °C, dye concentration = 100 mg/L).

Wool sample no.	Tensile strength (Newton/cm ²)	
	untreated wool	treated wool
1	1.234	2.124
2	1.044	1.456
3	0.758	1.112

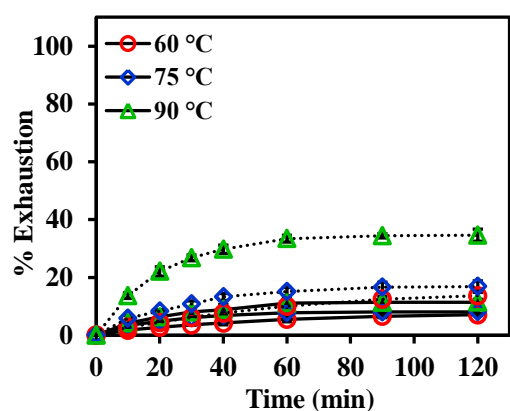
Table 2. Wrinkle and Wrinkle % of untreated and AgNPs-treated wool fabrics (Temp. 90 °C, dye concentration = 100 mg/L).

Wool sample no.	Wrinkle in raw wool	Wrinkle in dyed untreated wool	Wrinkle loss (%)	Wrinkle in dyed treated wool	Wrinkle loss (%)
1	37	33	10.8	29	21.6
2	34	30	11.8	26	23.5
3	31	28	9.7	23	25.8

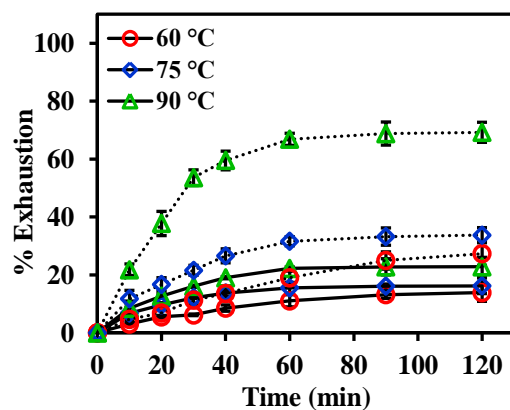
Table 3. Color measurements of untreated and AgNPs-treated wool fabrics (Temp. 90 °C, dye concentration = 100 mg/L).

Wool sample	Color values				Color intensity K/S	Color fastness			
	L*	a*	b*	ΔE		Wash	light	Perspiration	
								Acidic	Alkaline
Raw wool	-	-	-	-	-	-	-	3-4	3
Untreated dyed wool	30.66	24.00	17.00	55.95	17.33	3-4	4	3-4	3
Treated dyed wool	33.36	44.94	19.07	66.20	22.30	4-5	5	4-5	4

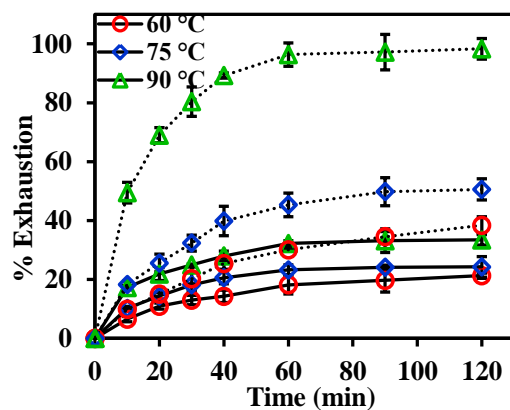
L* where (100 = white, 0 = black), a* where (positive = red, negative = green), b* where (positive = yellow, negative = blue).



(a)



(b)



(c)

Fig. 7. Exhaustion isotherm of (a) 50 mg/L, (b) 100 mg/L, and (c) 150 mg/L AR 18 in the untreated wool (—) and AgNPs-treated wool fabric (....)

3.3.2. Dyeing rate parameters

Several basic physicochemical parameters were varied to examine the rate of adsorption of dye by fibers. The most practical parameters were calculated in this analysis, i.e., the dyeing rate constant (k), diffusion coefficient (D), and the diffusion activation energy (E_{Diff}).

3.3.2.1. The rate constant of dyeing (k)

To determine the dyeing levels, wool samples were dyed in baths containing 50, 100, and 150 mg/L dye (Fig. 7a, b and c, respectively) at 60, 75, and 90 °C temperatures and 50:1 L:R. Before the fibers were immersed in the dye bath, the dye bath was heated to the dyeing desired temperature. The experimental data were analyzed using the pseudo-first- and second-order models, Elovich model, and kinetic intraparticle propagation model. With the application of the pseudo-first-order kinetic model (Eq.3), the values of k_f and q_e shown in Table 4 were calculated from the slope of the $\ln(q_e - q_t)$ vs. t draw. Figure 8 shows weak values of R^2 at different temperatures, suggesting the inapplicability of the pseudo-first-order model for the study of the AR18 adsorption kinetics for wool fabric. This inapplicability was further corroborated by the discrepancy at the equilibrium time between the experimental data and

the quantities of adsorption measured with the model. An irregularity was also observed in the change in the pseudo-first-order rate constant k_1 as the temperature rose (Table 4).

The pseudo-second-order model's linear integrative form is Eq.4, where k_2 (mg/g.min) is the constant of the pseudo-second-order adsorption rate. The half adsorption time ($t_{0.5}$) was calculated according to the rate constant and the kinetic parameters defined in table 4. Figure 9 shows the adsorption data fitted to varying temperatures using the pseudo-second-order kinetic model. The pseudo-second-order model provided the best correlation coefficient for all experimental data ($R^2 > 0.997$), and the calculated q_e , cal values were consistent with the experimental data of q_e , exp. These findings show that the experimental data for the AR 18 dye adsorption kinetics in the wool sample fit the pseudo-second model, which was confirmed by tests with three dye concentrations (50, 100, and 150 mg/L). The kinetic parameters for the adsorption of AR 18 varied by temperature, and the results show that the lowest constant rate (k_2) and original adsorption rate (hi) values were associated with the longest $t_{0.5}$, which could be explained by the presence of a thin wax protective layer on the wool surface and the resulting barrier action for the propagation of colors into the interior of the fiber [41]. The dyeing rate, amongst other kinetic mechanisms such as the boundary layer or film propagation effects, can be controlled using intraparticle propagation. Weber and Morris were the first to present the intraparticle propagation model, Eq.5 [42]; C is the intercept, k_p represents the intraparticle rate constant, and k_p was measured from the slope of the draw of q_t (mg/g) vs. $t_{0.5}$ (Fig. 10). The values for k_p are shown in Table 4. According to these results, because of the great driving power, the increase in the diffusion rate was associated with a

rise in the primary dye dosage. If the linear relation plot of q_t vs. $t_{0.5}$ crosses the origin, the intraparticle propagation characterizes the rate-control point. However, it is obvious from Fig. 10 that the linear graphs do not traverse their origins. As a result, the adsorption rate may have been influenced by other mechanisms (it was not only dependent upon intraparticle propagation) [43]. The Elovich equation refers primarily to the chemisorption phase. Equation 6 is often valid for heterogeneously adsorbed systems, where α and β for any experiment are constants. During each experiment, α is the primary adsorption rate (mg/g min), and β is the desorption constant (g/mg). The constant can be obtained from the slope and the intercept of the draw of q_t vs. $\ln t$ (Fig. 11). The values of constants β and α are collected in Table 4.

3.3.3. Coefficient of propagation and energy activation

Table 5 shows that the propagation coefficient of the dye increased with increasing temperature. This may be correlated with the swelling of the wool, which enhances the surface of adsorption and the propagation; thus, it is easier for AR 18 to penetrate. This can also be explained in terms of hydrophobic endothermic interactions. The obtained data show that the variability of the wool chains improved by AgNPs enhanced significantly with temperature. The involvement of AgNPs on the wool surface contributed to a significant rise in the number of adsorbents sites by forming salt bridges and complex links, which significantly enhances the interactions between wool fabric and AR18. The energy of activation can be calculated from the relation between $\ln D$ vs. $1/T$ (Eq.8).

The activation energy defines the propagation coefficient's dependence at the dyeing temperature and reflects the energy gap to the wool fabric that the dye molecule must surmount. The small energies of activation have a physical adsorption signature (5-40 kJ/mol), whereas larger energies of activation (40-800 kJ/mol) reveal chemical adsorption [44]. The energy of activation of AR18 dye in the

untreated wool fabric was 13.95 kJ/mol (Table 5), which suggests the process of physisorption. The corresponding activation energy was diminished in wool fabric treated with AgNPs. This can be demonstrated in terms of the decrease in the opposition of the wool fabric to the propagation of the dye and the further relaxation of the wool fabric treated with AgNPs [45].

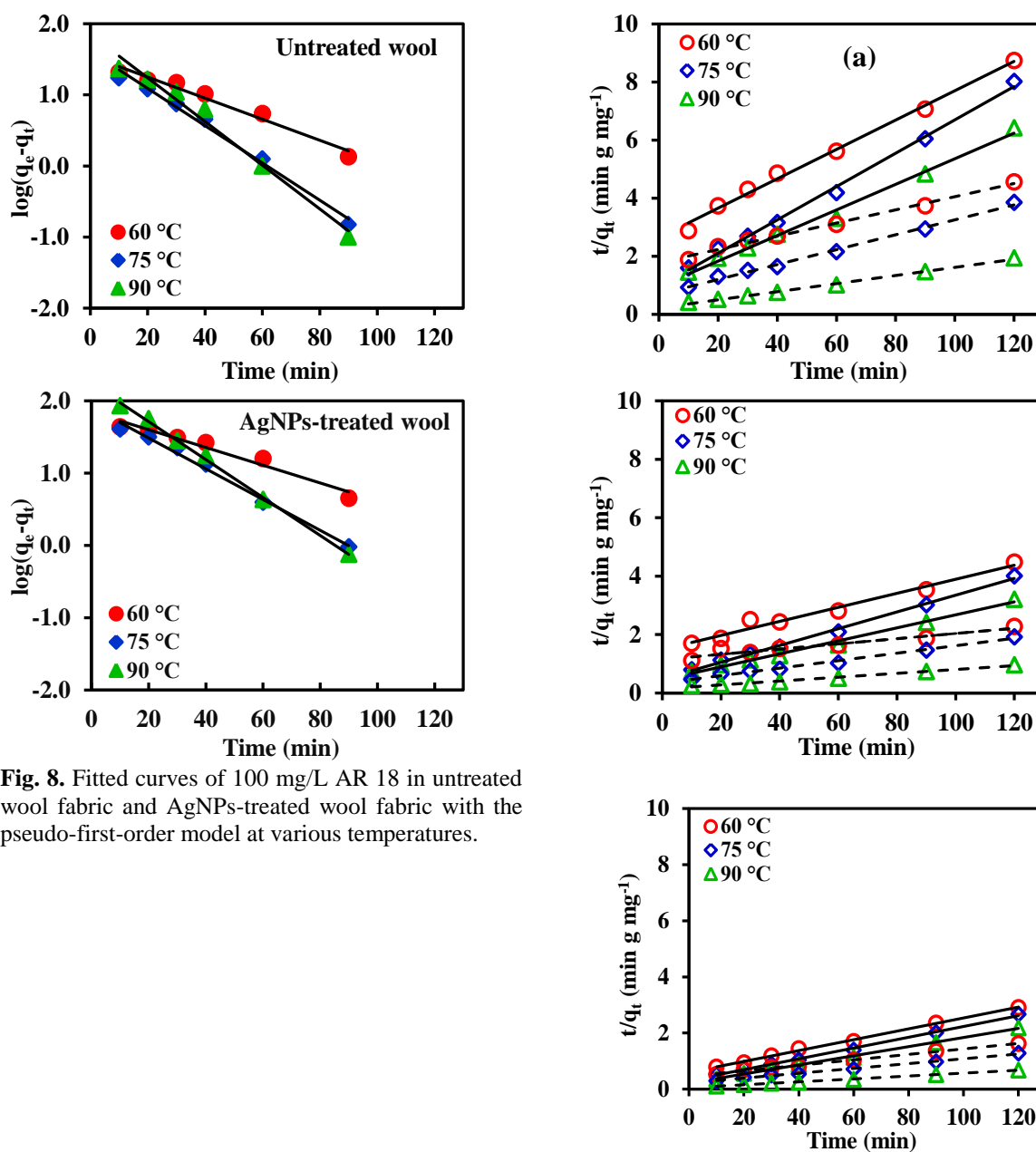


Fig. 8. Fitted curves of 100 mg/L AR 18 in untreated wool fabric and AgNPs-treated wool fabric with the pseudo-first-order model at various temperatures.

Fig. 9. Fitted curves of AR 18 at concentrations of (a) 50 mg/L, (b) 100 mg/L, and (c) 150 mg/L in untreated wool fabric (—) and treated wool (.....)

with the pseudo-second-order model at various temperatures.

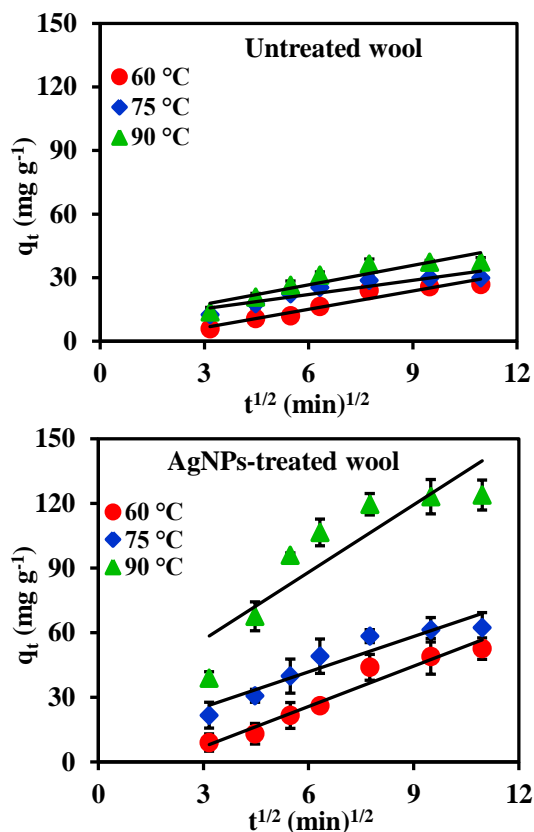


Fig. 10. Fitted curves of 100 mg/L AR 18 in untreated and AgNPs-treated wool fabrics with the intraparticle propagation model at various temperatures.

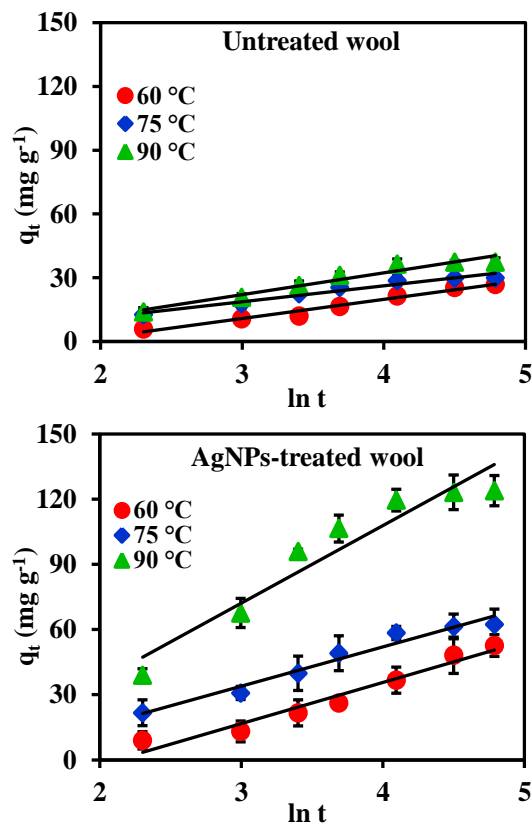


Fig. 11. Fitted curves of 100 mg/L AR 18 in untreated and AgNPs-treated wool fabrics with the Elovich model at various temperatures.

Table 4. Kinetic parameters for the adsorption of 100 mg/L AR18 onto wool fabrics at various temperatures.

Fabric	Temp. °C	Pseudo-First Order Model					Pseudo-Second Order Model					
		$q_{e,exp}$ mg/g	q_e calc. mg/g	K_1 , 1/min	R^2	$t_{0.5}$ min.	$q_{e,exp}$ mg/g	q_e calc. mg/g	$k_2 \times 10^3$ g/mg/min	h_i (mg/g·min)	R^2	$t_{0.5}$ min
Untreated wool fabric	60	0.03	0.03	0.04	0.89	16.9	26	32	1.3	1.3	0.99	24.0
	75	0.04	0.04	0.06	0.90	11.6	30	35	1.7	2.1	0.99	16.8
	90	0.06	0.07	0.08	0.87	9.8	37	45	2.0	4.0	0.99	11.1
Treated wool fabric	60	0.05	0.05	0.04	0.90	18.7	46	63	4.2	1.6	0.99	37.8
	75	0.06	0.08	0.05	0.88	14.1	62	78	4.9	3.0	0.99	26.2
	90	0.12	0.17	0.06	0.91	11.6	124	152	5.8	13.3	0.99	11.3
		Intraparticle propagation Model			Elovich Model							
		K_p (mg/g/min ^{1/2})	C (intercept)	R^2	β (g/mg)	α (mg/g/min)	R^2					
Untreated	60	4.00	-4.091	0.999	135	0.0026	0.9645					

wool	75	4.12	-0.501	0.998	133	0.0028	0.9533
fabric	90	5.47	-3.529	0.999	97	0.0044	0.9494
Treated	60	6.86	-10.046	0.993	68	0.0033	0.9805
wool	75	8.62	-6.484	0.990	56	0.0059	0.9635
fabric	90	22.15	-30.384	0.987	28	0.0134	0.9208

Table 5. Propagation coefficient and propagation activation energy of AR18 in untreated and AgNPs-treated wool fabrics at various temperatures.

Fabric	Temp. °C	$D_T \times 10^{10}$ (cm ² /s)	E_{Diff} (kJ/mol)
Untreated wool fabric	60	8.79	13.95
	75	9.58	
	90	10.00	
Treated wool fabric	60	9.84	11.02
	75	12.34	
	90	16.11	

3.4. Thermodynamic parameters

The thermodynamic parameters are given in Table 6. A very important thermodynamic factor is the dye's normal affinity ($\Delta\mu^0$) to the fabric substrate in the dyeing solution. This parameter can be described as the difference between the dye's chemical potential in fabric and in the dyeing solution [46]. The calculated value describes the dye's propensity to shift from its normal solution state to its default fabric state. It is noted from Table 6 that the variations in the normal affinity of dye molecules to untreated and treated wool fabrics are due to differences in the chemical structures and physical properties of the fabrics. There was a large increase in the normal AR18

affinity values in the treated wool fabric in comparison to that of AR18 in untreated fabric.

The values of ΔH° and ΔS° were determined from the slope and intercept of the linear plot of $\ln K_d$ versus $1/T$ (equation 11). As shown in table 6 the positive values of ΔH° and ΔS° indicate that the dyeing process is an endothermic and is spontaneous at higher temperatures [47]. Increasing dyeing temperature would promote the dyeing process. The positive ΔS° values indicate the randomness at fiber-dye solution interface, reflecting the affinity of dye towards the fiber. The higher positive value of ΔS° in case of AgNPs treated wool fabric confirms the higher affinity of dye towards the treated fabric.

Table 6. Thermodynamic parameters for the adsorption of AR18 onto untreated and AgNPs-treated wool fabrics at various temperatures.

Fabrics	Temp. °C	$-\Delta\mu^0$ (kJ/mol)	ΔH^0 (kJ/mol)	ΔS^0 (J/mol/K)
Untreated Wool fabric	60	5.69	21.36	80.87
	75	6.57		
	90	8.13		
Treated Wool fabric	60	7.61	65.74	218.74
	75	9.37		
	90	14.26		

3.5. Antibacterial activity of AgNPs-treated wool fabric

Antibacterial actions of untreated and AgNPs-treated wool against both *E. coli* and *S.*

aureus bacteria were investigated (Fig. 12). The antibacterial properties are as a result of Ag⁺ ions or free radicals on the surface of silver nanoparticles. The results demonstrate that the introduction of

AgNPs to wool fabric enhanced its antibacterial activity significantly. This change could be due to variations in the chemical composition, AgNPs size distribution, and mechanism of interaction with the wool fabric during treatment process. The antibacterial mechanism is often due to (1) the contact among Ag⁺ and phosphorous DNA groups of the bacterial cell structure; (2) the contact between Ag⁺ and sulfur-containing DNA- amino acids; (3) the concentration and repetition of the DNA strand structure; and (4) the Ag- catalyst effect of the interaction of water oxygen [48]. For assessing the antibacterial activity, three wool fabrics are shown in Fig. 12. It is noticed that the untreated wool fabric (1)

shows clear growth of bacteria with zero reduction percent R% against the two selected organisms, which indicates that the untreated fabric does not inhibit the bacterial activity, on the other side, the dyed untreated wool fabric (2) exhibits antibacterial activity scoring 6.65 and 10.25 R% values against the gram-negative and gram-positive bacteria, respectively. This may be due to the presence of various functional groups in AR18. The dyed treated wool fabric (3) scored 96.44 and 94.78 towards S.aureus and E.coli, respectively. This indicates that the AgNPs-treated fabric outstanding toxicity towards two selected organisms [49].

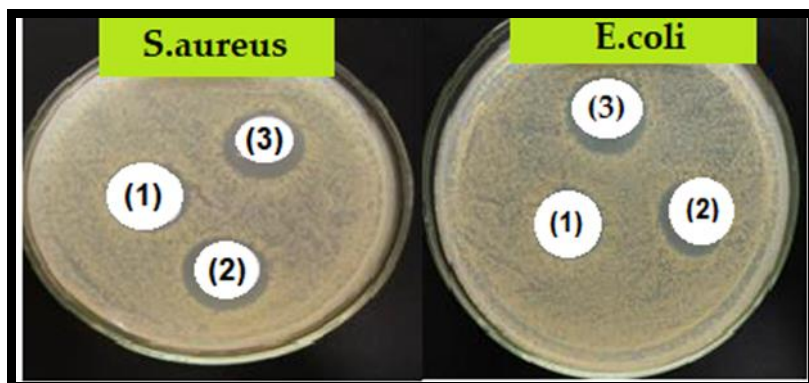


Fig. 12. Antibacterial activity of untreated fabric (1), dyed untreated fabric (2) and dyed AgNPs-treated wool fabric (3)

Conclusion

AgNPs can be suitably applied on wool fabrics to produce shades having good color strength. Wool fabric specimens modified with AgNPs shows good

physical properties than normal samples (color resistance and luminosity and the ability to wash). AgNPs treatment produces a wool fabric with advanced antibacterial properties enabling them to improve human health care and decrease the environmental impacts and fabric damage.

References

1. Clark, M. Fundamental principles of dyeing. Handbook of Textile and Industrial Dyeing, 2011, 3-27.
2. Martí, M., Barsukov, L. I., Fonollosa, J., Parra, J. L., Sukhanov, S. V., Coderch, L. Physicochemical aspects of the Liposome–Wool interaction in wool dyeing. Langmuir, 2004, 20(8), 3068-3073.
3. Warren S.P. Textile. Coloration and Finishing. Beijing: China Textile Press. 2004.
4. Kang J.Y. and Sarmadi M. Textile Plasma Treatment Review – Natural Polymer-Based Textiles. AATCC Review; 2004, 10, 28-32.
5. Albrecht M.A., Evan C.A., Raston C.L. Green chemistry and the health implications of nanoparticles. Green Chem. 2006, 8, 417.

6. Liu Y., Hussain M., Memon H., Yasin S. Solar irradiation and Nageianagi extract assisted rapid synthesis of silver nanoparticles and their antibacterial activity. *Digest J. Nanomaterials and Biostructures*. 2015, 10 (3), 1019–1024.
7. Memon H., Yasin S., Khoso N. A., and Memon S., “Study of wrinkle resistant, breathable, anti UV nanocoated woven polyester fabric,” *Surface Review and Lett.* 2016, 23(3), article 1650003.
8. Memon H., Kumari N., W.Jatoi A., and Khoso N. A., “Study of the indoor decontamination using nanocoated woven polyester fabric,” *International Nano Letters*, 2017, 7(1), 1–7.
9. Memon H. and Kumari N., “Study of multifunctional nanocoated cold plasma treated polyester cotton blended curtains,” *Surface Review and Letters*, 2016, 23(5), article 1650036.
10. Memon H., Yasin S., Khoso N. A., and Hussain M., “Indoor decontaminating textiles by photo catalytic oxidation—a review,” *J. Nanotechnol.*, 2015, Article ID 104142, 9 pages.
11. Dowling D.P., Betts A.J., Pope C., McConnell M.L., Eloy R., and Arnaud M. N. “Anti-bacterial silver coatings exhibiting enhanced activity through the addition of platinum,” *Surface and Coatings Technol.*, 2003, 163-164, 637–640.
12. Yuan Gao, & Cranston, R. Recent advances in antimicrobial treatments of textiles. *Text. Res. J.*, 2008, 78(1), 60-72.
13. Beer, C., Foldbjerg, R., Hayashi, Y., Sutherland, D. S., & Autrup, H. Toxicity of silver nanoparticles—Nanoparticle or silver ion? *Toxicology Letters*, 2012, 208(3), 286-292.
14. Greulich, C., Braun, D., Peetsch, A., Diendorf, J., Siebers, B., Epple, M., and Köller, M. The toxic effect of silver ions and silver nanoparticles towards bacteria and human cells occurs in the same concentration range. *RSC Advances*, 2012, 2(17), 6981.
15. Lee, S., & Jun, B., Silver nanoparticles: Synthesis and application for Nanomedicine. *International J. Molecular Sci.*, 2019, 20(4), 865.
16. Cañamares, M.V., Garcia-Ramos, J.V., Gómez-Varga, J.D., Domingo, C., Sanchez-Cortes, S. Comparative study of the morphology, aggregation, adherence to glass, and surface-enhanced Raman scattering activity of silver nanoparticles prepared by chemical reduction of Ag⁺ using citrate and hydroxylamine. *Langmuir*, 2005, 21(18), 8546–8553.
17. Pillai Z.S. and Kamat P.V. What factors control the size and shape of silver nanoparticles in the citrate ion reduction method? *J. Phys. Chem. B*; 2004, 108, 945–951.
18. Guesmi, A., Hamadi, N. B., Ladhari, N., & Sakli, F. Dyeing properties and colour fastness of wool dyed with indicaxanthin natural dye. *Industrial Crops and Products*, 2012, 37(1), 493-499.
19. Kubelka, P., Munck, F., A contribution to the optics of paint coatings, e.g (Ein Beitrag zur Optik der Farbanstriche). *Z. Tech. Phys.* 1931, 12, 593-601.
20. Alver, E., and Metin, A.Ü. Anionic dye removal from aqueous solutions using modified zeolite: Adsorption kinetics and isotherm studies. *Chemical Eng. J.*, 2012, 200-202, 59-67.
21. Ho, Y., & McKay, G. Pseudo-second order model for sorption processes. *Process. Biochemistry*, 1999, 34(5), 451-465.
22. Tayade, P. B., & Adivarekar, R. V. Adsorption kinetics and thermodynamic study of Cuminumcyminum L. dyeing on silk. *J. Envir. Chemical Eng.*, 2013, 1(4), 1336-1340.
23. AL-Othman, Z., Ali, R., & Naushad, M. Hexavalent chromium removal from aqueous medium by activated carbon prepared from peanut shell: Adsorption kinetics, equilibrium and thermodynamic studies. *Chemical Eng. J.*, 2012, 184, 238-247.
24. Ofomaja, A. E., Naidoo, E. B., & Modise, S. J. Kinetic and pseudo-second-Order modeling of lead Biosorption onto pine cone powder. *Industrial & Eng. Chemistry. Res.*, 2010, 49(6), 2562-2572.
25. Pang XY and Gong F. Study on the adsorption kinetics of acid red 3B on expanded graphite. *Journal of Chemistry*. 2008, 5, 802–809.
26. Feres-Comelo M. Thermodynamics and kinetics of dyeing and dye bath monitoring systems. *Handbook of Textile and Industrial Dyeing*; 2011, pp.184-206.
27. Chairat, M., Rattanaphani, S., Bremner, J. B., & Rattanaphani, V. An adsorption and kinetic study of Lac dyeing on silk. *Dyes and Pigm.*, 2005, 64(3), 231-241.
28. Samanta AK, Agarwal P and Datta S. Physico-chemical studies on dyeing of jute and cotton fabrics using jackfruit wood extract: Part II-dyeing kinetics and thermodynamic studies. *Indian J Fiber Text Res.* 2008; 33, 66–72.
29. Çalışkan N, Kul AR, Alkan S, Adsorption of zinc (II) on diatomite and manganese-oxide-modified diatomite; A kinetic and equilibrium study. *J. hazmat.* 2011, 193, 27–36.
30. Natsuki J and Abe T. Synthesis of pure colloidal silver nanoparticles with high electroconductivity for printed electronic circuits: The effect of amines on their formation in aqueous media. *J. Colloid. Interf. Sci.* 2011; 359, 19-23.
31. Öklem, T., Özdoğan, E., Namlığöz, S. E., Öztarhan, A., Tek, Z., Tarakcioglu, I. & Karaaslan, A. ‘Investigating the applicability

- of Metal Ion Implanation Technique (MEVVA) to Textile Surfaces', *Text. Res. J.*, 2006, 76(1), 32-39.
32. Scimeca M., Bischetti S., Lamsira H.K., Energy Dispersive X-ray (EDX) microanalysis: A powerful tool in biomedical research and diagnosis. *Eur J Histochem.* 2018; 62, 2841.
 33. Gomaa, E.H., Hilal, N.M., Abo Faraha, S.A. Improvement of Dyeing and Antimicrobial Properties of Cotton Fabrics through Pre-treatment with Silver Nanoparticles. *Egypt. J. Chem.* 2020, 63 (4), 1205 – 1217.
 34. Barani, H., Boroumand, M.N., Rafiei, S. Application of Silver Nanoparticles as an Antibacterial Mordant in Wool Natural Dyeing: Synthesis, Antibacterial Activity, and Color Characteristics. *Fibers and Polymers.* 2017, 18 (4), 658-665.
 35. Jiang, X.C., Chen, C.Y., Chen, W.M., Yu, A.B. Role of Citric Acid in the Formation of Silver Nanoplates through a Synergistic Reduction Approach. *Langmuir.* 2010, 26 (6), 4400–4408.
 36. Parvinezadeh, M. Katozian, B. Shaver, M. Clay nanoadsorbent as an environmentally friendly substitute for mordants in the natural dyeing of carpet piles. *Color. Technol.* 2014, 130, 54.
 37. Zhang, X.F., Liu, Z.G., Shen, W., Gurunathan, S. Silver Nanoparticles: Synthesis, Characterization, Properties, Applications, and Therapeutic Approaches. *Int. J. Mol. Sci.* 2016, 17(9), 1534-1568.
 38. Perumalraj, R. Effect of Silver Nanoparticles on Wool Fibre. *International Scholarly Research Notices.* 2012, 1-4.
 39. Al-Etaibi A.M. and El-Asasery, M.A. Dyeing of polyester with disperse dyes: Part 3. Characterization of ZnO nanoparticles treated polyester fabrics for antibacterial, self-cleaning and UV protective" *Int. J. Chem. technol. Res;* 2016, 9, 162-169.
 40. Al-Etaibi A., Alnassar H., and El-Asasery A. Dyeing of Polyester with Disperse Dyes: Part 2. Synthesis and Dyeing Characteristics of Some Azo Disperse Dyes for Polyester Fabrics, *Molecules;* 2016, 21, 855-861.
 41. Wei, B., Chen, Q., Chen, G., Tang, R., & Zhang, J. Adsorption properties of Lac dyes on wool, silk, and nylon. *J. Chemistry,* 2013,1-6. doi:10.1155/2013/546839.
 42. Raji F and Pakize M. Study of Hg(II) species removal from aqueous solution using hybrid ZnCl₂-MCM-41 adsorbent. *Appl. Surf. Sci;* 2013, 282, 415–424.
 43. Ghaedi M, Sadeghian B, Kokhdan SN. Study of removal of Direct Yellow 12 by cadmium oxide nanowires loaded on activated carbon. *Mater. Sci. Eng.* 2013, 33, 2258–2265.
 44. Nollet, H., Roels, M., Lutgen, P. Removal of PCBs from wastewater using fly ash, *Chemosph;* 2003, 53, 655-665.
 45. Mashaly, H.M., Moursy, N.S.1., Kamel, M.M. Dyeing of Antibacterial FINISHED Wool Fabric Using Ag/TiO₂ Nanocomposite Particles. *Int. J. Eng. Res. & Sci. & Tech.* 2014, 3, 4.
 46. Tang, B., Yao, Y., Chen, W., Chen, X., Zou, F., Wang, X. Kinetics of dyeing natural protein fibers with silver nanoparticles. *Dyes and Pigments,* 2018, 148, 224-235.
 47. Tayade, P.B. and Adivarekar, R.V. Adsorption kinetics and thermodynamic study of Cuminum cyminum L. dyeing on silk. *Journal of Environmental Chemical Engineering.* 2013, 1, 1336–1340.
 48. Yoon, K.Y., Byeon, J.H., Park, J.H., Antimicrobial characteristics of silver aerosol nanoparticles against *Bacillus subtilis* bioaerosols. *Environ Eng Sci.* 2008, 25, 289-293.
 49. Mohamed, A.A., Fouda, A., Elgamel, M.S., Hassan, S.E., Shaheen, T.I., Salem, S.S. Enhancing of Cotton Fabric Antibacterial Properties by Silver Nanoparticles Synthesized by New Egyptian Strain *Fusarium Keratoplasticum* A1-3. *Egypt. J. Chem.* 2017, 63 -71.

تحسين صباغة أقمشة الصوف عن طريق المعالجة بجسيمات الفضة النانوية

هيام محمد محمود، أسرار جمعة امام

قسم الكيمياء، كلية العلوم، جامعة الأزهر (بنات)، مدينة نصر، القاهرة، مصر

تعتبر الجسيمات النانوية مادة جديدة ناجحة لمعالجة الألياف والمنسوجات. في هذا العمل، تم تصنيع جسيمات الفضة النانوية (AgNPs) عن طريق الاختزال ومن ثم فحصها. تم استخدام الجسيمات النانوية المُصنَّعة لمعالجة وتحسين سطح النسيج، ثم تم صبغ القماش باستخدام C.I. Acid Red 18 (AR 18) عند درجات حرارة مختلفة. تمت دراسة الخواص الفيزيائية وقوة الشد ومعدل التجعد وقوة اللون وثبات الألوان للتعرق في نسيج الصوف المصبوغ المعالج وأقمشة الصوف الخام. وقد وجد أن الألياف المعالجة بالجسيمات النانوية كانت أقوى من الخيوط غير المعالجة. تم تحليل معدل الامتزاز وحسابه وفقاً لقوانين الحركة المختلفة. علاوة على ذلك، تم حساب معاملات الانتشار وطاقة التنشيط والمعاملات الديناميكية الحرارية.

ينتج العلاج باستخدام جسيمات الفضة النانوية (AgNPs) نسيجًا صوفيًا يتميز بثبات الألوان وخصائص مضادة للبكتيريا مما يتيح رعاية صحية عالية وتقليل للتأثيرات البيئية.